Isotopic effects on the level density and symmetry energy: an experimental perspective

M. D'Agostino[1], F. Gulminelli[2], Ad. Raduta[3], F. Gramegna[4], M. Bruno[1], G. Baiocco[1], L. Bardelli[5], S. Barlini[5], M. Bini[5], F. Cannata[1], G. Casini[5], M. Chiari[5], M. Cinausero[4], M. Degerlier[4], E. Geraci[1], V. L. Kravchuk[4], T. Marchi[1], P. Marini[1], P. Maurenzig[5], L. Morelli[1], A. Nannini[5], P. Napolitani[2], A. Olmi[5], A. Ordine[6], G. Pasquali[5], S. Piantelli[5], G. Poggi[5], V. Rizzi[4], A. Stefanini[5], G. Vannini[1]
(NUCL-EX collaboration)

(1) Dipartimento di Fisica dell'Università and INFN, Bologna,Italy,
(2) LPC Caen IN2P3-CNRS/EnsiCaen et Universitè, Caen, France,
(3) NIPNE, Bucharest-Magurele, POB-MG 6, Romania,
(4) INFN, Laboratori Nazionali di Legnaro, Italy,
(5) Dipartimento di Fisica dell'Università and INFN, Firenze, Italy,
(6) INFN, Sezione di Napoli,Italy,

Abstract We propose an experimental campaign with the ALPI-Tandem accelerator at LNL, aimed at backtracing primary fragments formed in multifragmentation reactions from the asymptotically (cold) measured ones. This is a necessary step for the experimental determination of the symmetry energy at finite temperature and/or sub-saturation density, which is one of the research themes to be explored with stable and (future) radioactive beams, such those delivered by SPES at LNL. As a side goal, this study will allow to put constraints on the pairing effects on the level density.

The devices we plan to use for these measurements are Garfield [1] (installed at LNL) and some ancillary detectors [2].

The proposed experimental campaign is motivated by the results obtained by our previous experiments, performed with Garfield at the ALPI-Tandem accelerator at LNL. We are presenting to this PAC a letter of intent, instead of a proposal, for two reasons.

The first one is that the Garfield set-up needed for the nearly-4π measurement of fragments and light charged isotopes requires to disassembly the present set-up, dedicated to measure light charged particles, heavy residues and γ's, used for experiments performed in February 2008. Since two additional experiments on γ-emission will be presented to this PAC, planning to use Garfield in the present set-up, we decided to postpone the Garfield re-assembling to the beginning of 2009.

The second motivation is that, to properly backtrace the decay of hot fragments, we need to increase the granularity of the forward part of Garfield for isotope detection (as justified in detail in the following). This implies to replace the CsI detectors in the forward angular region with a more granular array of stopping detectors. This improvement will require an additional request of funds to the I.N.F.N. 3^{rd} Scientific Committee (June-September 2008). If this request is approved, some time is needed to buy and mount the new detectors. We plan to have Garfield ready for the proposed experiments starting from the beginning of 2009.

In the case of a positive answer by the PAC to this letter of intent, we will present a beam time request to next PAC meeting.

1 The physical motivation

Strong experimental and theoretical studies have been recently undertaken, with the aim of investigating the modifications of the symmetry energy of bulk matter as well as finite nuclei with respect to normal density and zero temperature evaluations. Left panel of Fig.1, taken from ref. [3], shows different independent evaluations in nuclear matter of the density dependence of the symmetry energy using various experimental observables (isospin diffusion, neutron skin thickness, isoscaling, giant resonances, pre-equilibrium emission). Right panel of Fig.1, taken from ref. [4], shows the status of the art for the theoretical predictions. It is clear that a considerable effort is still needed to pin down the isovector part of the nuclear equation of state.

Such information plays a key role in determining properties of neutron rich nuclear matter in neutron star crusts [5, 6], as well as cooling properties of proto-neutron stars [7, 8, 9].

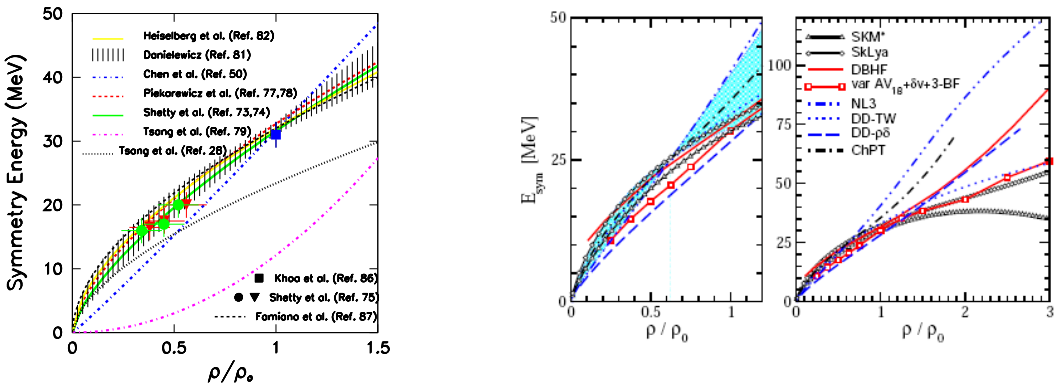

Figure 1: *Left: Comparison between the results on the density dependence of the symmetry energy obtained from various experimental studies from ref. [3]. For details, see [3] Right: Symmetry energy as a function of density predicted by different microscopic calculations. The left panel shows the low-density region, while the right panel displays the high-density range. The figure is taken from Ref. [4].*

It has been theoretically shown that the symmetry energy of an excited nucleus C_{sym} (sometimes also indicated as E_{sym} in the literature) can be directly probed in the evaporative regime from the so called isoscaling parameter, measuring the relative production yield of a given isotope in two reactions involving nuclei of similar masses and different isospin ratios [10]. In reactions at intermediate energies, this same isoscaling parameter has been tentatively used to extract information about the density dependence of the symmetry energy [11, 12, 13]. Another recently proposed observable is the width of the isotopic distributions of primary fragments, which has been predicted to be directly related to C_{sym} [14, 15] both if fragmentation occurs at equilibrium or out of equilibrium [16].

While the fragmentation regime is needed to probe the symmetry energy at sub-saturation densities, the temperature dependence of C_{sym} around saturation, at moderate to high temperatures is presently a subject of debate [9, 17, 18, 19] and can be

investigated with relatively low-energy beams, such those delivered by ALPI.

However, extracting quantitative information about the symmetry energy at finite temperature from experimental observables is a hard task: secondary decays of excited primary fragments can distort signatures contained in primary fragment isotopic distributions. Previous studies at intermediate incident energies have shown that these primary unstable fragments can be characterized by excitation energies up to 3 MeV/nucleon before they undergo secondary decays [20]. By means of low-energy beams we may be able to observe the decay of compound nuclei at similar excitation energies. The back-tracing of these decays will then provide information on the more complex problem of secondary decays in fragmentation phenomena.

In particular we expect that close to the multifragmentation threshold, the produced fragments will be relatively cold. The experimental reconstruction through correlation techniques of secondary decays in such moderately excited fragments will allow us to trace back the primary fragmentation pattern minimizing the model dependence of the procedure.

Level densities at low excitation energy are known to exhibit important isotopic and odd-even effects, resulting in staggering effects in different isotopic observables. The proposed back-tracing through correlations will therefore also address the problem of quantitatively understanding such effects; in particular an experimental constraint of excited levels population should help disentangling the influence of the binding energy and the level density in the observed staggering.

To better justify these goals, we made specific calculations with the statistical microcanonical model MMM [21], for sources predicted to be formed in central collisions for the reactions $S + Ni(isotopes)$ at $E_{beam} \approx 14.5A\ MeV$, measured at ALPI in our previous experiments with Garfield [22].

2 Measurements with Garfield and model predictions

We present hereafter some results coming from the reactions $^{32}S +^{58,64} Ni$ at an incident energy $\approx 14.5A\ MeV$ (corresponding to $\approx 3.3\ A\ MeV$ centre-of-mass energy), measured with the Garfield device. For these reactions Garfield covers the centre-of-mass angles up to $\sim 120^o$, with a geometrical efficiency larger than 80%, and energy thresholds for charge identifications smaller than 1 AMeV. In the first experiment, performed in 2002, fragments and light charged particles were identified in charge on the whole apparatus, but the mass identification was restricted to the laboratory angular range $6^o \div 18^o$. After very successful tests performed in 2002, the GARFIELD apparatus was equipped in 2006 with digital electronics [23], allowing mass identification up to 150^o for light fragments.

To select events corresponding to central collisions, we adopted the method of the "shape analysis" [24], common to other intermediate and high energy experiments performed with $\simeq 4\pi$ detectors [25, 26]. We then selected "well detected events", where at least 70% of the total charge was collected (dashed line of Fig.2), and we examined different regions of the "flow angle", corresponding to different sphericity of the events. The bump below the selection line corresponds to the detection of the quasi projectile ($Z = 16$).

Well detected events, for $\theta_{flow} \leq 30^o$ show the presence of a heavy residue. By looking

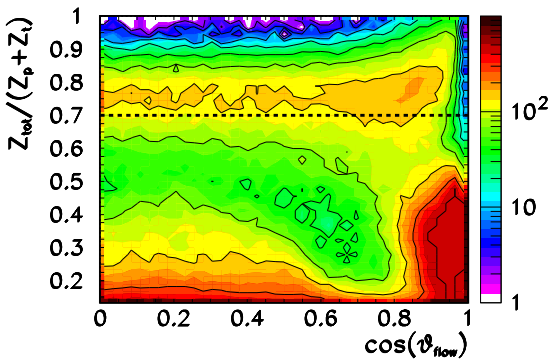

Figure 2: *Ratio of the total detected charge to the entrance channel charge as a function of* $cos(\theta_{flow})$. *Line at 70% represents the required condition for subsequent analyses.*

at charge partitions for increasing θ_{flow}, we have observed a decrease of the largest fragment and the appearance of nearly equal-size 3-fragments events . We selected central events as those characterized by $\theta_{flow} \geq 60^o$ [25].

Measured central events (see Fig.3, left panel) are very similar to those predicted by the statistical model MMM [21] for the decay of a source formed in an incomplete fusion of the projectile and target ($Z_{source} = 40$, $A_{source} = 82$ for the n-poor reaction and 87 for the n-rich one), at an excitation energy close to the center- of-mass energy (middle and right panels of Fig.3). Both for data and model predictions two classes of events can be identified: events where all detected products have a charge $Z < 30$, hereafter noted as fragmentation-like events (upper part of fig.3), and events containing a heavy residue with $Z \geq 30$, hereafter noted evaporation-like (lower part of fig.3).

The comparison between data and microcanonical predictions (Fig.3) can be at this stage only qualitative. Not only because predictions are not filtered through the software replica of the experimental apparatus, but also because probably the experimental data do not correspond to a sharp microcanonical ensemble but to a superposition of results coming from sources differing in size and excitation energy. To backtrace the most probable distribution of source characteristics not only average quantities have to be taken into account, but also fluctuations.

With this caveat in mind, model predictions add however important knowledge to the characterization of the events in this energy range. Due to the low excitation energy of the source and the high Q-value and Coulomb energies required to create many-fragment partition, the energy remaining as internal excitation energy of primary fragments is very different in many-fragments events and in evaporation events. This is shown in Fig.4.

The model predicts that break-up fragments produced in many-fragments events have an average internal excitation energy of about 1.25 AMeV, while the heavy residue and light fragments produced in evaporation events can be excited up to 2 AMeV. This shows that low-energy reactions can be extremely useful in the quest of the temperature and density dependence of C_{sym}. On one side, selecting many-fragment events, we can study low-density partitions similar to the ones produced in fragmentation phenomena at much higher beam energies, but with considerably reduced distortions due to secondary decay. Indeed due to the low internal excitation energy, it will be possible to at least partially reconstruct the secondary evaporation pattern in a model-independent way, as

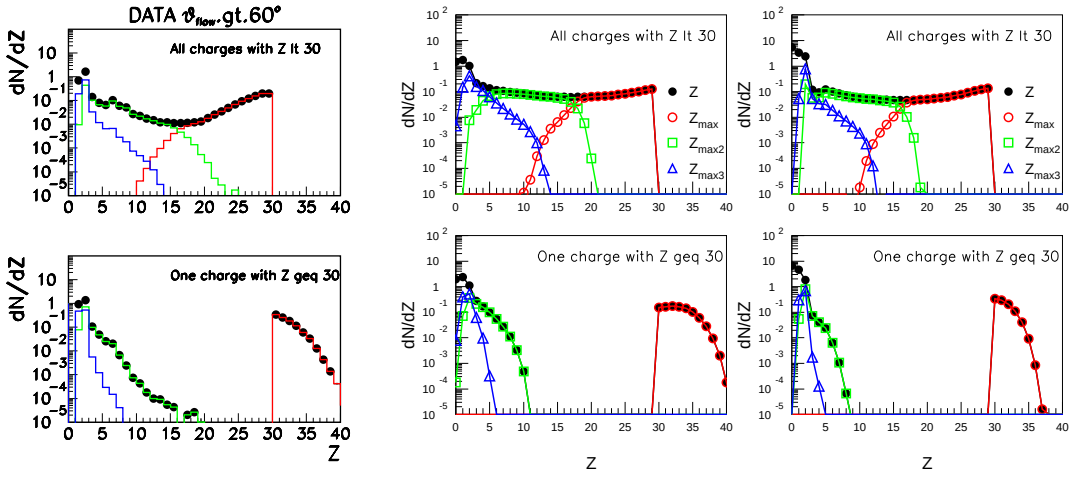

Figure 3: *Left panels: measured charge distribution (symbols) and charge of the 3 largest products as red, green and blue lines respectively. Middle panels: Charge distribution (black symbols) and charge of the 3 largest products (as red, green and blue symbols, respectively) for primary fragments as predicted by MMM. Right panels: As the middle panels, but for asymptotic fragments.*

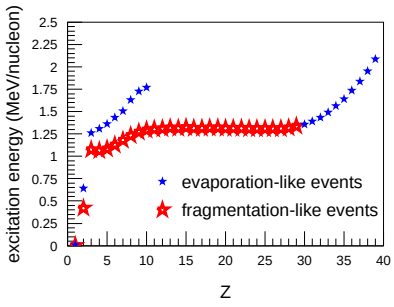

Figure 4: *Excitation energies of primary fragments for evaporation-like events ($Z_{max} \geq 30$) and multifragmentation-like events (all fragments with $Z < 30$) as predicted by MMM.*

we develop at length in the following paragraph. On the other side, selecting evaporation events, we can access more excited primary fragments in well-controlled experimental conditions. The back-tracing of their secondary decay made by detailed comparison with evaporation models will allow to validate evaporation corrections needed to interpret data in the high-energy multifragmentation regime. In particular, understanding the competition among different open channels and how the fragment N/Z composition evolves during the evaporation chain can significantly improve our search for signatures of the symmetry energy in nuclear reactions.

The other difficulty in C_{sym} measurements concerns the reliability of the different algorithms proposed to extract C_{sym} from evaporation-corrected observables. Indeed these algorithms are derived using simplifying assumption of neglecting mass and energy conservation. These approximations can be estimated by statistical model calculations. We show in Fig.5 the symmetry energy calculated for evaporation and multifragmentation

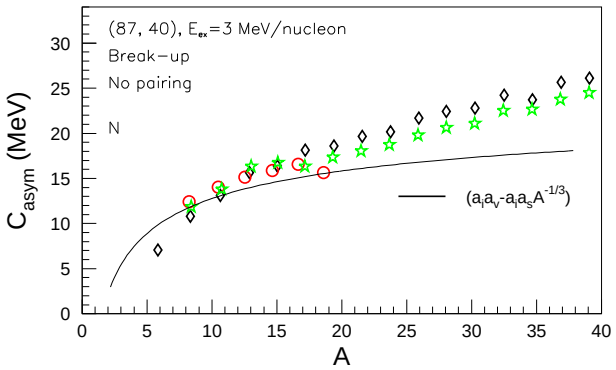

Figure 5: *MMM simulations. Open diamonds: Symmetry energy calculated with relation(1) for break-up fragments. Open circles represent the calculation for evaporation-like events ($Z_{max} \geq 30$) and open stars for multifragmentation-like events (all fragments with $Z < 30$). Full line: input C_{sym} of the model.*

events via the formula suggested in Ref. [15]:

$$\sigma^2(A)|_Z \approx < A > T/(2C_{sym}(A)) \quad (1)$$

The black curve represents the input value of C_{sym} implemented in the model, to be compared with the estimation from break-up isotopic widths eq.(1) [14]. The agreement with the input value of C_{sym} appears very good for both classes of events for fragments of size $8 \leq A \leq 20$. In particular a better agreement with the expected value of C_{sym} is provided by the "evaporation-like" events, because of less serious effects due to mass-charge conservation.

We pass now to examine the experimental isotopic observables, to be employed for the C_{sym} evaluation. We will see that these observables show so strong Z-odd-even effects, that very accurate experimental and theoretical investigations are needed to access the symmetry energy.

3 Z-odd-even anomalies

The Z-odd-even effect has been observed in several experiments where a good accuracy of Z-identification is achieved. An enhancement in even-Z fragments has been observed from spontaneous fission to the breakup of AGeV heavy projectiles [27, 28, 29, 30] [1].

The anomaly seems to be independent of the beam energy and of the acceptance of the experimental devices (angular acceptance), but slightly decreasing with increasing number of neutron of the reaction partners. It seems more pronounced in the mass 58 reactions, in particular in n-poor systems, while it has not been observed in reactions involving stable Ca projectile and targets. Pairing effects acting in the last steps of the evaporation chain only partially explained this anomaly [27, 28, 29, 30].

To evaluate the relationship of the Z-odd-even effect to the isospin and to deconvolute the effect from the exponential behaviour of Z-distribution, the ratio of the yield of fragments from the n-poor reaction to the yield of fragments from a more n-rich reaction can be considered.

[1] For a review of experiments with signatures of fine structure in the measured yields see Table I of Nucl.Phys. A733 (2004) 299

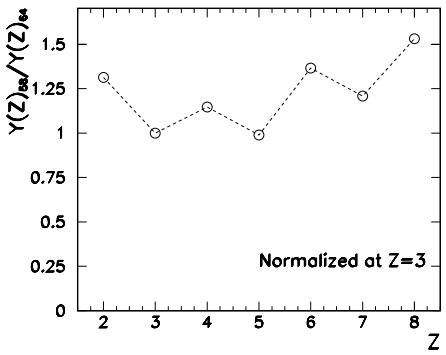

Figure 6: *Ratio of the measured yields in the reactions* $^{32}S +^{58} Ni$ *and* $^{32}S +^{64} Ni$. *The ratio is normalized to 1 at* $Z = 3$.

We show in Fig.6 the ratio of the measured yields in the reactions $^{32}S +^{58} Ni$ and $^{32}S +^{64} Ni$. By considering the normalization of the data at $Z = 3$, we see a staggering effect of the order of 10-20%, in favour of even-Z as observed also in Ref.s [27, 28, 29, 30].

Another kind of odd-even oscillations develops, for adjacent charges, either in the isospin ($I = N - Z$) or equivalently in the $< N > /Z$ behaviour as a function of Z (Fig.7), as well as in the variance of the mass distribution (Fig.8). In principle these

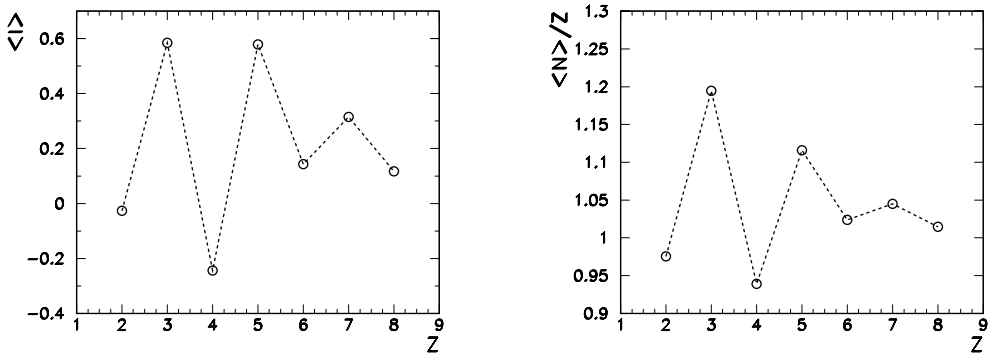

Figure 7: *Isospin* $< I >=< N - Z >$ *and average neutron to proton ratio* $< N > /Z$ *as a function of the fragment charge for the reaction* $^{32}S +^{58} Ni$.

effects can be explained from the odd-even gap in the nuclear binding energies, even Z-nuclei being more stable than odd Z, and even-N being more stable than odd N.

However, if we look at model predictions with a pairing term included in the binding energy parametrization (Fig. 9), we can see an effect on the relative yields of Z-distributions, but isotopic widths appear essentially unaffected, contrary to the experimental result.

It has been recognized in previous studies [32] that different physical effects contribute to the staggering. If the introduction of a Wigner isospin term [31] is certainly needed in the mass parametrization and will definitely reduce the predicted staggering especially for heavy fragments, important effects are also expected in the structure of both discrete and continuum excited levels also because of the pairing interaction.

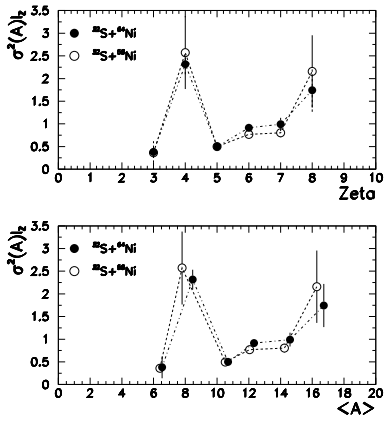

Figure 8: *σ^2 of the A-distribution, for fragments with Z from 3 to 8, as a function of the charge (top) and of the average mass (bottom).*

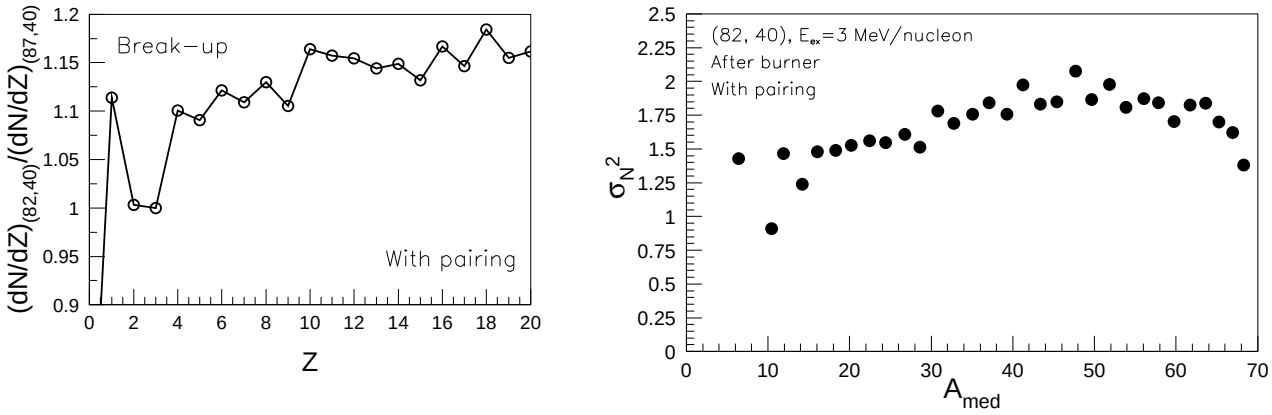

Figure 9: *MMM simulations. Left: Ratio of the charge distributions of a n-poor to a n-rich source. Right: σ^2 of the A-distribution. The pairing contribution to the masses is taken into account.*

Indeed the preferential presence of low-lying discrete particle-unstable levels in odd-even isotopes should favor the population, in the last step of the evaporation chain, of even-even isotopes, thus enlarging the isotopic distribution for Z-even. The backshift of continuum levels in even isotopes will also modify the decay properties of even isotopes respect to odd ones. It is known [32] that deconvoluting the effects of the binding energy and the effects of the density of states is not simple. Experimental observables on the structure and population probability of the excited levels are therefore very important. Such observables are discussed in the next section.

4 Low-lying resonances

An especially interesting situation where the decay pattern of an excited fragment and the associated excited states structure can be experimentally probed is the case of low-lying resonances. Such states are dominant in the last step of evaporation chains, and therefore we expect that an experimental evaluation of their contribution can explain

a large part of the staggering effects, and at the same time give a strong constraint on evaporation models helping to disentangle binding energy properties from level density properties.

Experimentally, the observation of kinetic energy spectra of evaporated particles (see Fig.10), characterized by Maxwellian shapes are usually employed [33] to disentangle

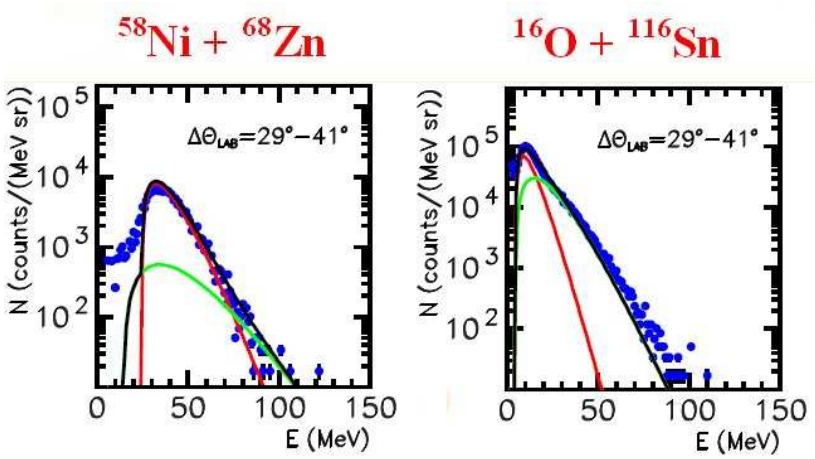

Figure 10: *α-particle kinetic energy spectra. Black line represents a 2-moving sources fit, to disentangle preequilibrium and equilibrium contribution. Red line represents the thermal contribution, green line the preequilibrium one (from Ref. [33].*

pre-equilibrium effects and equilibrium evaporations. In particular the observation of similar slopes for different particle species is a signature of statistical emission.

However, kinetic energy spectra represent inclusive observables constructed by collecting in the same spectrum particles emitted in different events. These single-particle analyses provide limited information, since the correlations between successive particles emitted in the same event are lost. Especially in the study of excited nuclei, these correlations can be particularly important.

In particular, these inclusive observables are insufficient to guarantee a model independent correction of secondary decay nor to control staggering effects, as needed to pin down the behavior of C_{sym}. For example, N/Z asymmetric nuclei at moderate excitation energies are expected to display spectroscopic features and decay modes that cannot be predicted by the Weisskopf theory [27].

A study of the de-excitation of compound nuclei by means of correlation techniques can help to explore the N-Z-dependence of de-excitation processes and perform stringent tests of the theories of statistical decay.

To this aim, for the reactions $^{32}S + ^{58,64}Ni$ 14.5 AMeV incident energies, we built correlation functions of the relative momentum, for all the measured pairs of isotopically resolved fragments and particles. The existence of well defined excited primary fragments can be evidenced from enhancements of the relative momentum distribution.

One can define [34] the two-fragment relative momentum correlation function as:

$$1 + R(q_{rel}) = C\frac{Y(q_{rel})}{Y_{back}(q_{rel})} \tag{2}$$

where $q_{rel} = |\vec{q_i} - \vec{q_j}|$ is the relative momentum of fragments i and j; $Y(q_{rel})$ and $Y_{back}(q_{rel})$ are the coincidence and background yields for fragment pairs of relative momentum q_{rel}

and $C = N_{back}/N_{coinc}$ where N_{coinc} and N_{back} are the total number of coincidence and background pairs. The background yield is constructed by means of the mixed event technique.

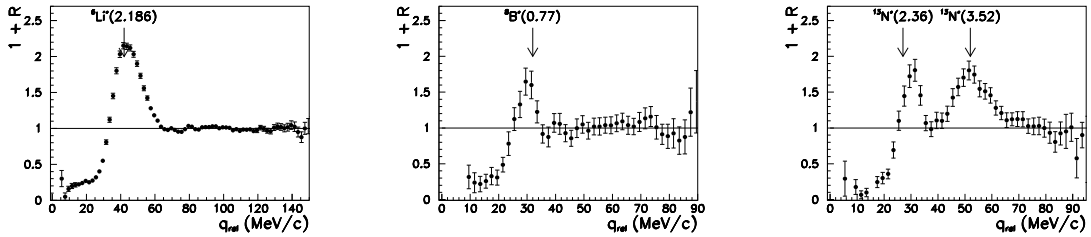

Figure 11: *From left to right: $d-\alpha$ ($^6Li^*$ 2.186 MeV), $p-^7Be$ ($^8B^*$ 0.77MeV), $p-^{12}C$ ($^{13}N^*$ 2.35, 3.52 MeV) correlation functions.*

We show in Fig.11 some examples of correlation functions of pairs of isotopes, showing charged particles and fragments emitted by excited states of primary fragments ($^6Li^*$, $^8B^*$, $^{13}N^*$, respectively). Peaks in the correlation functions were observed for other pairs, like for instance (p,α) or $(d,^3He)$ from $^5Li^*$ and $(^3He,^4He)$ from $^7Be^*$, for a total of 23 observed resonances from $^4He^*$ to $^{19}F^*$ and excitation energies up to $\sim 1.5A\ MeV$ (see upper part of fig.13).

By performing Gaussian fits of the relative momentum distribution (see Fig.12), for each observed resonance we extracted the probability for the considered pair to initially belong to an excited fragment.

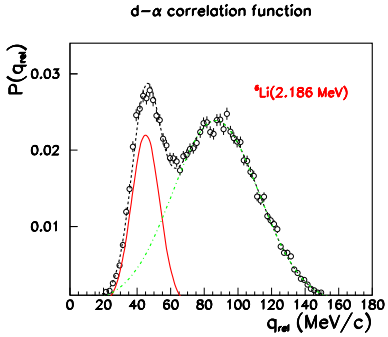

Figure 12: *Symbol: relative momentum probability distribution for a pair (d,α). The black line represents the global fit, the red line is the resonating contribution ($^6Li^*$ 2.186 MeV), the green line is the phase space background.*

Finally from these probabilities, we built the weighted average probability for a pair of isotopically resolved fragments to be originated by a discrete level of an excited fragments (lower part of Fig.13).

This study neglects all decays involving not detected free neutrons. However neutron-unstable levels are not numerous in this mass domain [35].

From this analysis it results that an odd-even Z-anomaly is observed also for primary fragments, showing that the decay of a Z-odd fragment is more probable that the decay of a Z-even one. Furthermore, by analyzing the observed resonance-decays, we noticed that in more than one-half of the observed decays, odd-Z primary fragments decay by

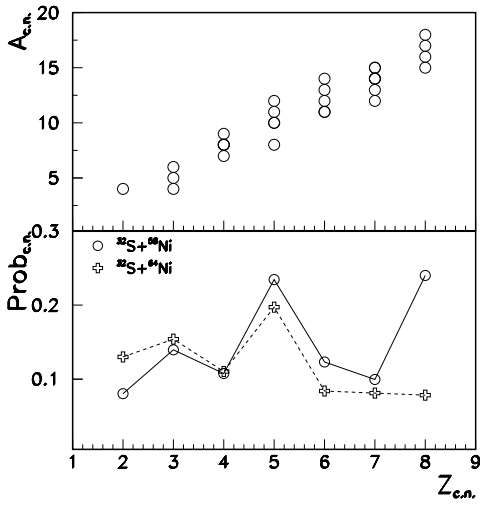

Figure 13: *Top panel: observed resonances for an excited fragment of charge Z_{cn} and mass A_{cn}. Bottom panel: average measured probability for a pair to be originated by a resonance-decay of a nucleus of charge Z_{cn}.*

proton (deuteron) emission, while even-fragments decay by α-particle emission. This (at least partially) could explain the odd-even-Z anomaly of the asymptotic distributions shown in Fig.6. Unfortunately these qualitative results are not sufficient to convincingly constrain the level density and disentangle binding energy effects from level density effects. Indeed the granularity of the present apparatus leads to an insufficient angular resolution to recognize all resonances (nuclear tables contain 38 levels in the considered energy range [35]). Only an improved granularity and a systematic exploration of odd-even effects and resonance population in nuclei differing in isospin will allow to strongly constrain the interplay between isospin, temperature, and pairing effects on the level density.

5 Efficiency issues

We recall here that the correlation functions were initially built just to check the energy calibration quality. Indeed, if the energy calibration is wrong even only by few percent, or the pedestal is not carefully measured, or the Delta-E detector thickness is not well measured, the relative momentum is distorted and the resonance peak can be dramatically enlarged and lost in the uncorrelated background.

In general the decay of $^8Be_{g.s.} \rightarrow \alpha + \alpha$ is used to this purpose, due to its separation from the background yield (see Fig.14).

Encouraged by the good result obtained in this case, we looked at other resonances, despite the low granularity of the apparatus (initially built to detect fragments and particles in low multiplicity events).

To be more quantitative in future experiments, we studied how much the granularity of the forward detector limitates the detection of resonance-decays and it deforms the correlation peaks.

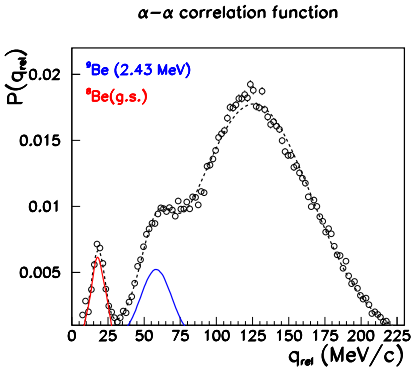

Figure 14: *Relative momentum probability for $\alpha-\alpha$ pairs in the laboratory angular region $6^o \div 18^o$. ^8Be (ground state) and $^9Be \rightarrow ^8 Be + n \rightarrow \alpha + \alpha + n$ (2.43 MeV) decay contributions are represented as red and blue lines, respectively. The green line is the phase space background.*

We therefore performed simulations, by including in secondary decays some resonances: $p +^7 Li$ from $^8Be^*$ (17.64 MeV), $d + \alpha$ from $^6Li^*$ (2.186 MeV) and $t + \alpha$ from $^7Li^*$ (4.652 MeV), falling at different values of the relative momentum (~ 25, ~ 42 and ~ 83 MeV/c, respectively).

We show in Fig.15 the spectrum $d + \alpha$ from $^6Li^*$ for unfiltered events, for those filtered through the software replica of the actual experimental configuration [2] and finally through an improved forward array. For all the studied resonances the peak is

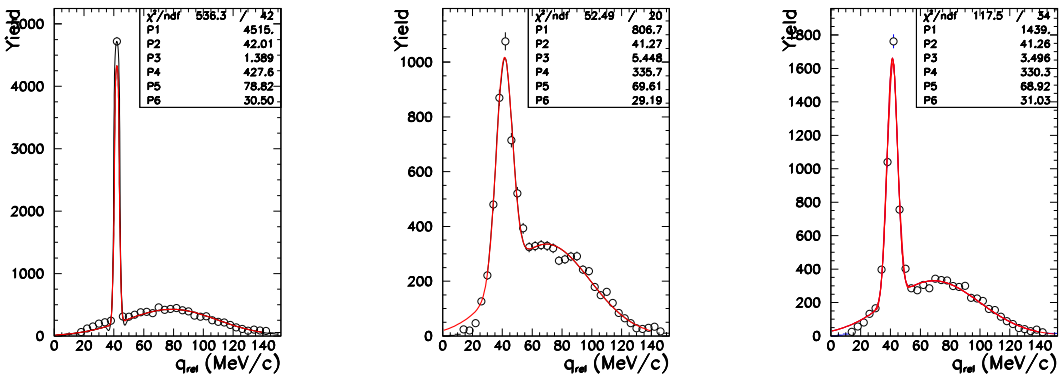

Figure 15: *Points: relative momentum distribution for a pair (d, α) in the laboratory angular region $6^o \div 18^o$. Left panel represents unfiltered simulation, middle panel the filtered distribution through the filter of the analyzed experiment, right panel shows the distribution in the case we increase by a factor 2 the granularity of the stopping detectors. P_1, P_2, P_3 represent the maximum, average value and σ of the resonance. P_4, P_5, P_6 the same observables for uncorrelated pairs.*

centered at the expected value, independently of the granularity used in the software filter. On the contrary a low granularity filter enlarges up to a factor 4 the resonance width.

By only doubling the number of the forward stopping detectors, the measure of the

width is improved by a factor 2. The reduction of the width is mainly due to double-hits recovering and this is an important point in order to disentangle correlated contribution from background.

As far as the overall efficiency is concerned, i.e. the ratio between the initial and the detected numbers of pairs in the laboratory angular region $6^o \div 18^o$, with an improvement of the forward array we could attain 80%.

6 Modification of the forward part of Garfield to improve performances

The forward part of the Garfield apparatus consists in the Ring Counter (RCo) [2], an annular detector designed to be centered at 0^o with respect to the beam direction. It is an array of three-stage telescopes realized in a truncated cone shape. The first stage is an ionization chamber (I.C.), the second a strip silicon detector (Si) and the last stage a CsI(Tl) scintillator. The RCo has eight separate silicon detectors, pie shaped, each one segmented into eight independent annular strips on the front surface. In front of each silicon detector there is a sector of a specially designed IC. Behind each silicon detector there are two CsI(Tl) crystals.

1. As shown in the previous section, by replacing the 16 CsI(Tl) scintillators with a larger number of crystals (from 32 to 64 crystals instead of 16), the granularity increases and the relative angle determination results more precise, greatly improving the measure of the relative momentum between isotopically identified fragments and therefore the backtracing of the excited-state decays.
   We are still studying the best number of crystals to be used in order to improve the performances while not severely increasing the complexity of the apparatus both from the mechanical and from the electronic side.

2. We plan to reverse mount the eight silicon detectors (one for each azimuthal sector). This would allow to identify the charge of fragments stopped in the Silicon detector via pulse shape and digital electronics. The Z identification of particles stopped in Silicon was up to now performed via DeltaE-E with analogic signals from the I.C. and the Silicon detector. Since we have only one I.C. per sector the simultaneous Z identification by two methods will allow to recover double hits in the I.C. of fragments impinging in different strips. Indeed, two particles impinging on the same sector of the I.C. are not disentangled by the DeltaE-E method, whereas the pulse shape can be performed in different strips of the Silicon detector. The I.C., mainly devoted to the detection of heavy residues and low-energy fragments, is still needed in order to keep the thresholds as low as possible.

7 Plan of requested time and beams

As discussed in the previous Sections, a deeper understanding of odd-even effects in the average observables (as the charge distribution) and in higher moments (as the width of mass distributions), is important to experimentally evaluate the symmetry energy from nuclear reactions which produce several intermediate mass fragments and light charged particles.

These odd-even effects were observed for a large variety of reactions and in few experiments this anomaly seems to be absent [27]. Therefore we plan to start our measurements initially by looking for the absence of the effect (e.g. with the $^{40}Ca+^{40}Ca$ reaction). Then we could perform other measurements by changing some characteristics of the reaction partners (like their neutron content or their charge) to find the onset of the odd-even anomaly.

A possible sequence of measurements could be:

- $^{40,48}Ca +^{40,48} Ca$
  in the case the effect is absent, we could increase the charge of the target, as in
- $^{40,48}Ca +^{58,64} Ni$
  we could also change the charge and isospin of the projectile, as in:
- $^{48}Ti +^{48} Ti$ or $^{48}Ti +^{58,64} Ni$

all these reactions, with ALPI beams of about 14-15 AMeV incident energies, would lead for central collisions to an almost completely fused systems with about 3 AMeV excitation energy.

The GARFIELD apparatus will be used, which has now not only the capability to measure the charge, the energy and the emission angles of nearly all the reaction products, but also provides information on the mass of the emitted charged products, being now equipped with digital electronics [23].

On the basis of previous experiments, we estimate that 12 days for each proposed reaction should allow to collect a sufficient number of isotopes in complete central events (with a fusion cross section of $200 \div 300$ mb, a pulsed beam of intensity ≈ 0.5 pnA and timing of ≈ 1 ns and a target thickness of about 200 μg/cm^2).

This would allow to calculate correlation functions between isotopes and to study in detail the secondary decays, to possibly get information on the symmetry energy.

We also need a couple of days of Tandem B, C, O beams, before the real measurements, with the aim of carefully calibrating the forward detectors. This is particularly important for the proper "detection" of excited states decaying via charged particles, as mentioned in the previous Sections. We also plan to perform measurements with radioactive sources, to properly set electronic thresholds and to have an additional point for energy calibration.

References

[1] F. Gramegna et al., Nucl. Instr. And Meth. A389 (1997) 474; F. Gramegna et al., 2004 IEEE Nucl. Science Symposium, Rome, 16-22 October 2004.

[2] A. Moroni et al., Nucl. Instr. And Meth. A556 (2006) 516.

[3] D.V. Shetty et al., arXiv:0704.0471v1 [nucl-ex] 3 Apr 2007

[4] C. Fuchs and H.H. Wolter, Eur. Phys. J. A 30, 5 (2006).

[5] J.Pethick et al., Ann. Rev. Nucl. Part. Sci. 45, 429 (1995).

[6] J.M.Lattimer et al., Astrophys. J. 550, 426 (2001).

[7] D.Page, arXiv:astro-ph/0405196.

[8] D.G.Yakovlev et al., arXiv:astro-ph/0409751.

[9] P.Donati et al., Phys. Rev. Lett. 72, 2835 (1994)

[10] M.B.Tsang et al., Phys.Rev. C64 (2001) 054615; M.B. Tsang et al., Phys. Rev. Lett. 86 (2001) 5023; A.S. Botvina, O.V. Lozhkin, W. Trautmann, Phys. Rev. C 65 (2002) 044610; G.A. Souliotis et al., Phys. Rev. C 68 (2003) 024605; W.A. Friedman, Phys. Rev. C 69 (2004) 031601(R); M. Colonna and M.B. Tsang, Eur. Phys. J. A 30, 165 (2006).

[11] W. P. Tan et al., Phys. Rev. C68, 034609 (2003).

[12] T.X. Liu et al., Phys. Rev. C 69, 014603 (2004).

[13] A.Ono et al., Phys. Rev. C70, 041604 (2004).

[14] Ad. R. Raduta and F. Gulminelli, Phys. Rev. C75, 024605 (2007).

[15] Ad. R. Raduta and F. Gulminelli, Phys. Rev. C75, 044605 (2007).

[16] C.Ducoin et al, Nucl.Phys. A 789 (2007) 403-425

[17] D.J.Dean et al., Phys. Rev. C66, 45802 (2002)

[18] A.Lefevre et al, PRL 94, 162701 (2005).

[19] J.Xu et al, arXiv:nucl-th/0609035.

[20] N.Marie et al., Phys. Rev. C58, 256 (1998); S. Hudan *et al.*, Phys. Rev. C67 (2003) 064613.

[21] Al. H. Raduta and Ad. R. Raduta, Nucl. Phys. A703, 876 (2002); F. Gulminelli, Ph.Chomaz, Al. H. Raduta, Ad. R. Raduta, Phys. Rev. Lett. 91, 202701 (2003).

[22] E. Geraci et al. Eur. Phys. J. Special Topics 150 (2007) 21.

[23] L. Bardelli et al., Nucl. Instr. and Meth. A 491, 244 (2002); L. Bardelli et al. Nucl. Instr. And Meth. A560 (2006) 517; G. Pasquali et al. Nucl. Instr. And Meth. A570(2007)126

[24] J. Cugnon and D. L'Ĥote, Nucl. Phys. A397 (1983) 519.

[25] N.Marie et al. Phys. Lett. B 391(1997) 15.

[26] M. D'Agostino *et al.*, Phys. Lett. 368 (1996) 259.

[27] L. B. Yang et al., Phys. Rev. C60, 041602 (1999) and references quoted therein.

[28] E. Geraci *et al.*, Nucl. Phys. A732 (2004) 173; Nucl. Phys. A734 (2004) 524.

[29] M. V. Ricciardi et al. Nucl.Phys. A733 (2004) 299; P. Napolitani et al., Phys. Rev. C 70 (2004) 054607; P. Napolitani et al. Internat. Journal of Modern Physics E - Nucl. Phys. 13 (2004) 333; P. Napolitani et al. Phys. Rev. C 76 (2007) 064609; D. Henzlova et al. arXiv nucl-ex/0801.3110v1.

[30] W. Trautmann Nucl. Phys. A 787 (2007) 575c.

[31] P. Moller, J.R. Nix, W.D. Myers, and W.J. Swiatecki, At. Data Nucl. Data Tables, 59, 185 (1995).

[32] K. H. Schmidt and W. Morawek, Rep. Prog. Phys. 54 (1991) 949; A. V. Ignatyuk Yad. Fiz. 29 (1979) 875 and Sov.J. Nucl. Phys. 29 (1979) 450; S. Steinhauser et al. Nucl. Phys. A 634 (1998) 89; A. R. Junghans and Benlliure Eur. Phys. J. A 13 (2002) 93.

[33] S. Barlini et al., submitted to Nucl. Phys. A

[34] R. Trockel *et al.*, Phys. Rev. Lett. **59** 2844, (1987);
M. A. Lisa, W. G. Gong, C. K. Gelbke, and W. G. Lynch, Phys. Rev. **C44** 2865, (1991).

[35] http://www.tunl.duke.edu/nucldata/